Available online at www.sciencedirect.com
ScienceDirect
Procedia Engineering 158 (2016) 33 – 38
Procedia Engineering
www.elsevier.com/locate/procedia

VI ITALIAN CONFERENCE OF RESEARCHERS IN GEOTECHNICAL ENGINEERING – Geotechnical Engineering in Multidisciplinary Research: from Microscale to Regional Scale, CNRIG2016

X-ray Computed Tomography for capillary collapse of loose unsaturated sand

Mariagiovanna Moscariello[a], Simon Salager[b], Sabatino Cuomo[a,]*

[a]*Università degli Studi di Salerno, Via Giovanni Paolo II, 132, 84084 Fisciano (SA), Italy*
[b]*Université Grenoble Alpes, Laboratoire 3SR, BP 53, 38041 Grenoble, France*

Abstract

The collapse of unsaturated soils consists of the reduction in volume upon wetting at constant total stress. Several studies at the macro scale outline the influence of initial void ratio, confining pressure and matric suction on the onset of collapse of standard laboratory specimens. Conversely, few observations at the micro scale are available in the literature, although the influence of the particles arrangement and intergranular bonding has been formerly supposed. The collapse of fine sand derived by a pyroclastic soil of Southern Italy is investigated in this paper at the microscale using the X-ray Computed Tomography. The experimental procedure, formerly tested on similar pyroclastic soils, consists into testing a remoulded specimen (only loaded by its self-weight), which undergoes a reduction of matric suction until the collapse occurs. The laboratory investigation aims to: i) follow the transformation of the particles arrangement; ii) measure the global variations of the specimen in terms of water content, porosity and saturation degree during the wetting stage; iii) measure the local porosity, water content and saturation degree in several representative sub-volumes of the specimen. The experimental evidence outlines that the collapse occurs at very low suction while it is not mandatory to reach the complete saturation, emphasized by the presence of macro-voids at collapse.

Peer-review under the responsibility of the organizing and scientific committees of CNRIG2016

Keywords: Capillary collapse; X-Ray Computed Tomography; grain-scale investigation; characterisation at local and global scales

1. Introduction

The collapse is commonly defined as the irreversible decrease in total volume of a soil resulting from wetting at

* Corresponding author. Tel.: +39(0)89-964231; fax: +39(0)89-968732.
E-mail address: scuomo@unisa.it

Peer-review under the responsibility of the organizing and scientific committees of CNRIG2016
doi:10.1016/j.proeng.2016.08.401

essentially unchanging total vertical stress [1]. It occurs in granular soils, when capillary forces are of the same order of magnitude as other interparticle forces (i.e. skeleton forces, weight of particles), and when the particles arrangement is loose. Several authors studied the collapse at macro-scale, however, the capillary collapse at the grain scale and the modifications of the particles arrangement during the wetting process have been less observed [2].

In this paper, the mechanism of capillary collapse was investigated for a pyroclastic soil of Southern Italy using X-ray Computed Tomography, which is a non-destructive technique that allows visualizing the internal structure of a body through the measurement of density and atomic composition [3]. So far, the applications of the tomography to porous media have been mainly focused on: i) the analysis of porosity and fluid flow; ii) the evaluation of density, water content and volume fractions; iii) the characterization of the particles arrangement of asphalts and concretes [3]; iv) the characterization of the local deformations within a soil specimen in a mechanical testing device [3]. The paper is structured as follows: first, the experimental procedures and the tested soil are described; then, the results are discussed and compared to those achieved using standard methods; finally, some conclusions are drawn.

2. Materials and Methods

2.1. X-ray Computed Tomography

X-ray Computed Tomography (X-ray CT) transformed the field of experimental mechanics because of its ability to image the particles arrangement in opaque materials [4]. This technique applied to granular materials can evaluate properties usually available (as porosity, grain size distribution, water content), as well as those unavailable using standard laboratory techniques (as particle orientation, local variation of porosity, water content and saturation degree). X-ray CT provides morphological information of a sample at different scales, in non-destructive way, through the attenuation coefficients (i.e. the X-ray attenuation due to the bulk density) of the various materials [5]. The results are 2D or 3D images (radiographies) that map the variation of the attenuation coefficient inside the specimen. The experimental set-up allows detecting the photons, which are transmitted through the specimen, so that the basic components of the equipment are an X-ray source, a detector and a rotation system. The specimen is placed on the rotation stage, between the source and the detector. The source is composed by a sealed, solid-anode, micro-focus X-ray vacuum tube. The detector is a flat-panel used also for medical purposes.

The tomographic scan procedure can be summarizing as follow: the X-ray source generates a continuous X-ray beam, which passes through the specimen that rotates around its vertical axis at a controlled angular velocity. The X-ray-beam hits the detector [6], which converts the radiation in electric charge. The charge is passed to the computer and becomes a digital image. During the rotation, 8 radiographies are acquired and averaged at each of 1024 different angular station, so an entire scan requires about 2 hours.

For an unsaturated material, a good contrast among its three phases (solid, liquid and gas) is necessary in order to perform a successful scan; so an important step is the selection of proper parameters to perform the scan. The contrast is governed by the rotation speed of the plate and the waiting time before the acquisition of each radiography. Whereas, the acquisition time and the good quality of the resulting image are governed from the energy and the intensity of X-ray source, the filters and the number of radiographies.

2.2. Image processing procedures

The 3D representation of the inner structure of an object is reconstructed through the radiographies acquired while the specimen is slowly rotated. The 3D image is obtained implementing the back-projection through an algorithm which assigns to each point of the object the average value of all projections at the corresponding location. The image obtained is higher blurred than the real specimen, so it needs of a correction through the Filtered Back projection algorithms based on Fourier considerations [7].

In this paper, the reconstruction is carried out through the software DigiCT, which uses a reconstruction algorithm based on the FDK Algorithm [8]. For the reconstructed images, the distribution of the number of voxels as a function of their gray intensity can be plotted, and the graph is labelled histogram. The reconstructed images are then processed through segmentation procedure, which consists into labelling each voxel (volumetric pixel) based on the ratio of its gray value to a reference value [9]. There are many segmentation techniques proposed in the literature among which global thresholding, locally adaptive thresholding, probabilistic fuzzy clustering and region growing methods. Specific image segmentation techniques have been adopted for granular materials in which three phase are simultaneously present. Here, a segmentation based on the region growing technique is adopted for unsaturated sand and the procedure is implemented in the Matlab code. The region growing method is based on the assumption that all the voxels belonging to a particular object are connected and similar, i.e. the method recognizes that if a voxel is surrounded by other voxels of the approximately the same gray value, it should be considered as belonging to the same phase.

The procedure is interactive and composed of four steps: i) partial thresholding; ii) Partial Volume Effect (PVE) filtering; iii) simultaneous phase growing; iv) filling of interface. (i) The partial thresholding consists in defining the regions where each phase is present [9]. This can be done considering the histogram as composed of three Gaussian curves (one for each phase), and thresholding the gray values where the Gaussian curves are not overlapping. At this step, the peaks of the histogram are selected, in order to isolate the 50 % upper part of the grains Gaussian Curve, the 50 % lower part of the void Gaussian curve, while for the intermediate phase (water), the voxels belong to the interval included 25 % left and 25 % right starting from the peak of water Gaussian curve are isolated. The second step (ii) consists in the PVE filtering, i.e. the identification of voxels in which air and grains phases are taken into one voxel. The PVE is represented by the standard deviation, so a threshold filter of the standard deviation is applied in order to exclude PVE voxels. After the PVE filtering, the excluded voxels are re-set to color black and will be handled later. The simultaneous phase growing (iii) consists in filling the other half of each phase. New thresholds (tolerance thresholds) are selected equal to the partial threshold. This step defines the black (undefined) voxels without considering the interfaces, which will be handled in the final step of the procedure. (iv) The filling of interface, indeed, consists in determining the phase to which the remained voxels of the interfaces belonging. The neighbors of the remained voxels are used to determine their phase identity.

The results of trinarization are images in three gray values, which can be manipulated to extract the amount of voxels representing each phase. The histograms of these images gave three values of the number of pixels, which were labelled for air P_a, for water P_w and for grains P_g. The porosity (n) (Eq. 1), the water content (Eq. 2) and the degree of saturation (S_r) (Eq. 3) are evaluated through the numbers of pixels representing each phases as follows:

$$n = \frac{(P_g + P_w + P_a) - P_g}{P_g + P_w + P_a} \tag{1}$$

$$\theta = \frac{P_w}{P_w + P_a + P_g} \tag{2}$$

$$S_r = \frac{P_w}{P_w + P_a} = \frac{\theta}{n} \tag{3}$$

2.3. Tested soils

The material used for the tests was derived from an air-fall volcanic (pyroclastic) soil of Southern Italy, originated from the explosive activity of Vesuvio volcano, identified as “class A” by Bilotta et al. [10], and formerly studied by Bilotta et al. [10,11] and Cuomo et al. [12,13]. This pyroclastic soil is a natural sandy silt with 40 % to 60 % of Sand and 20 % to 60 % of Silt, and has the peculiarity to contain grains with internal voids so that the specific gravity (G_s) is quite small, typically from 2.33 and 2.59 [10].

The specimens were cylindrical, 10 mm high and 10 mm in diameter, for a total volume of 0.785 cm^3. Such a small size was necessary to obtain a high resolution of X-ray images (7.5×7.5×7.5 μm^3/voxel, expressed in terms of voxel size), necessary to distinguish each grain and internal voids partially filled with water. Also related to this issue were some constraints to the size of the grains to be possibly investigated. Particularly, artificial sand was derived from the natural pyroclastic soil, with median diameters equal to 200 μm, and a narrow grain-size distribution (150-250 μm) was selected by sieving. This choice was related to three contrasting requirements such as to have: i) grain sizes smaller than 600 μm to guarantee that the specimen could include a sufficient number of grains, that was about 1000-3000 in the specimens we used; ii) particles larger than 100 μm to make possible the individuation of each grain and surrounding menisci, since the minimum size of grains profitably investigated through X-ray CT technique was about 5 μm [6]; iii) a reasonable grading of grain sizes to preserve the structure of the original natural soil, thus having similar porosity.

The specimen preparation was aimed to obtain very loose materials, similar to natural undisturbed pyroclastic soils, i.e. with high porosity and “open” structure composed of macrovoids and aggregates of grains. To do so, the artificial sand was mixed to distilled water at 20 % in weight and sealed into a plastic container for 12 hours. The mixture was poured into the cell; the initial porosity of the specimen was 67.5 %, while the water content in weight was 20 %, which correspond to suction 1 kPa in the Soil Water Retention Curve of the sand tested.

3. Results and discussion

A wetting test using the X-ray CT was performed to investigate the capillary collapse of the fine pyroclastic sand. The test was carried out on remolded specimen with high initial porosity and initial volumetric water content 14 %. The specimen was saturated reducing the suction from 1 kPa up to the collapse (0.1 kPa) through four steps. Each suction decrement was kept constant at least for 8 hour in order to reach the equalization, and then a 3D image was acquired. The aims of this test are: i) follow the transformation of the particles arrangement in the specimen; ii) evaluate local porosity, water content and saturation degree in several representative sub-volumes; and iii) evaluate the global variations of water content, porosity and saturation degree during the wetting stage.

The initial particles arrangement (Fig. 1a) is an “open” characterized by high porosity and low interparticle strength. There are some aggregates of particles hold by water bridges due to the negative pressure of water, the water content is low. The decrement of suction up to 0.3 kPa produces an increment of capillary cohesion, which is defined as the force caused by surface tension and pressure difference across air-water interface that attracted the grains. At suction 0.3 kPa (Fig. 1b), the increment of capillary stress caused 11 % radial strain, the reduction of the number and the size of macro-voids and the formation of water clusters (defined by Scheel et al. [14] as the connected regions of wetting more than two grains). The decrease of suction up to 0.2 kPa, instead, does not produce any significantly modification of the particles arrangement (Fig. 1c). At suction 0.1 kPa, the collapse occurs and there is the rearrangement of the particles arrangement: the body forces become predominant and the capillary cohesion is not able to hold the grains. Indeed, the axial strain is about 34 %, while the radius of the specimen is already equal to 1 cm, so the radial strain is cancelled.

The analysis of the evolution particles arrangement conforms to the studies in literature, which indicate that the capillary cohesion depends on the liquid content at low saturation degree. The mechanical stiffness of the wet bridges and clusters decreases only for very large water content, corresponding to more than one half of the void space in the assembly being filled by liquid [14].

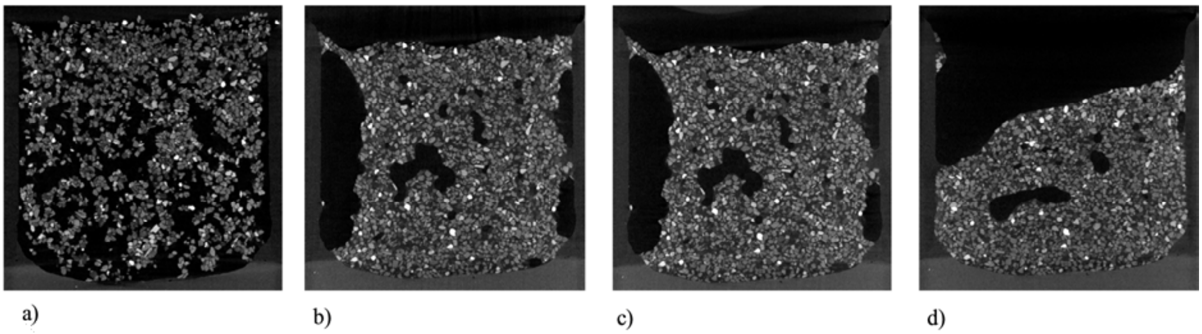

Fig. 1. X-ray CT images of the vertical section N°750 during the wetting test on fine sand: a) initial conditions; b) suction = 0.3 kPa; c) suction = 0.2 kPa and d) suction = 0.1 kPa (collapse).

The evolution of the particles arrangement upon wetting is also followed through the trinarized images, which is used to determine global and local porosity (n_{trin}), water content (θ_{trin}) and saturation degree, as shown in Sect. 2.2.

Figure 2 outlines the evolution of n_{trin} and θ_{trin}. The specimen does not experience significantly reduction of porosity down to suction 0.5 kPa. The measurements are then compared with that obtained through standard measurements. The standard porosity (n_{st}) is evaluated measuring the height of the specimen and its variation during the tests, while the strandard water content (θ_{st}) is evaluated at the beginning and at the end of the test: at the beginning the water content is known; at the end the specimen is weighed in wet conditions, and put into the oven for 2 hours, then it is weighed in dry condition. The highest relative error between the two types of measurement is 12.47 % for the porosity and 8.92 % for the water content, which can be considered acceptable.

The relative error is also evaluated for the volume of water and solid phase. The trinarized procedure underestimates the volume of water both at suction 1.0 kPa and at 0.1 kPa; while the volume of solid phase is underestimated at suctions 1.0 kPa and 0.5 kPa, is overestimated at suctions 0.2, 0.3 and 0.1 kPa. The relative errors can be attributed to: i) presence of “mixels” (i.e. voxels in which two or more phases are presents), which may alter the evaluation of the solid phase amount; ii) and, more importantly, inhomogeneties induced by wetting in the specimen. Moreover, for pyroclastic sand, the error can be also attributed to the presence of grains with low gray values close to water.

The relationship between water content versus matric suction is modelled using the Van Genuchten (1980) and Gardner (1958) equations. Van Genuchten equation describes the water retention data through four independent parameters (Eq. 4), where θ_s and θ_r represent the saturated and residual water content, respectively; α, β and m=1-1/β are empirical shape parameters.

$$\theta(s) = \theta_r + \frac{(\theta_s - \theta_r)}{\left[1 + (\alpha s)^{\beta}\right]^{m}} \tag{4}$$

The best-fitting parameters found for Van Genuchten model were: θ_s= 0.413, θ_r= 0.060, α= 6.295 and β=3.052. The model is able to well interpret the experimental evidence with R^2=0.8906. It is worth noting that these values are in agreement with those estimated by Cuomo et al. [12] for similar volcanic soils.

The trinarized images are used to evaluate the local porosity and the local water content, dividing the volume of the specimen in cylindrical sub-volumes (1 cm in diameter and height equal to 3 times the median diameter of the sand). Figure 3 shows the plots of local porosity and water content along the vertical; the dots are located at middle height of each sub-volume. At the initial conditions the sand has a linear distribution of the local porosity along the vertical, which is almost equal to that obtained at suction 0.5 kPa. The value of the global n is equal to the local porosity of the sub-volumes at the centre of the specimen, and lower at the top than at the bottom. Water content (θ) is linear with depth and the highest value belongs to the sub-volumes at the top of the specimen. At suction 0.3 kPa and 0.2 kPa, the local water content is almost equal to the global θ along the vertical, while the local porosity has an irregular trend. At the collapse, both local porosity and water content have a linear trend along the vertical.

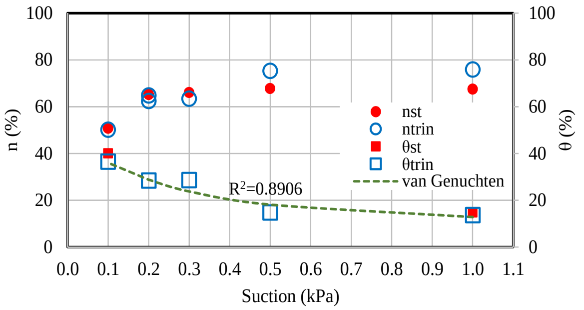

Fig. 2. Comparison among standard measurements (subscript st) and measurements obtained using trinarized images (subscrit trin) for water content (θ) and porosity (n).

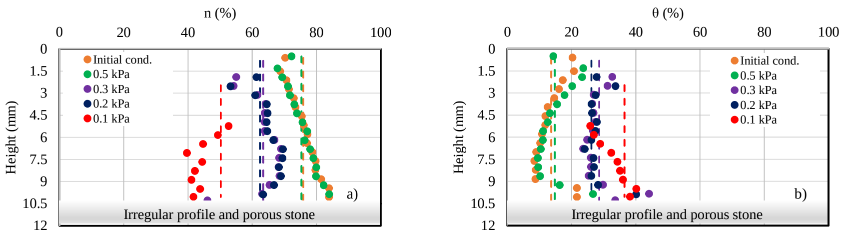

Fig. 3. Comparison among local and global porosity (a) and water content (b) evaluated through trinarized images. Dashed lines represent global measurements, dots local measurements. The dots are located at middle height of each subvolumes.

4. Concluding remarks

The capillary collapse of artificial loose unsaturated pyroclastic sand was analyzed through X-ray Computed Tomography. The effects of wetting process resulting in a change of the soil internal structure were measured. It was outlined the role played by the change of capillary cohesion which produced a remarkable radial strain. Porosity and water content were measured at global level for the whole specimen using standard techniques and at microscale for specific subvolumes using the trinarized X-ray images. The global and local measurements were compared and the differences were acceptable. Moreover, the local modification of soil internal structure induced by wetting were measured and analyzed towards the local changes and global behavior of the whole specimen.

Acknowledgments

This research activity was developed within the framework of 2014-2015 Erasmus+ European Project and 2015-2016 Galileo Project Campus France “Soil mechanical behaviour from grain to specimen scale laboratory testing: towards new sustainable mitigation works against flow-like landslides and similar phenomena related to climate change” Grant n. G15-110.

References

[1] E.C. Lawton, R.J. Fragaszy, j.H. Hardcastle, Stress ratio effects on collapse of Compacted Clayey sand. Journal of Geotechnical Engineering, ASCE 117(5) (1991) 714–730.
[2] J.F. Bruchon, J. M. Pereira, M. Vandamme, N. Lenoir, P. Delage, M. Bornert, Full 3D investigation and characterisation of capillary collapse of a loose unsaturated sand using X-ray CT. Granular Matter 15(6) (2013) 783-800.
[3] E. Andò, S.A. Hall, G. Viggiani, J. Desrues, P. Bésuelle, Grain-scale experimental investigation of localised deformation in sand: a discrete particle tracking approach. Acta Geotechnica 7(1) (2012) 1-13.
[4] I. Vlahinić, E. Andò, G. Viggiani, J.E. Andrade, Towards a more accurate characterization of granular media: extracting quantitative descriptors from tomographic images. Granular Matter 16(1) (2014) 9-21.
[5] A.C. Kak, M. Slaney, Principles of computerized tomographic imaging. New York: SIAM, 2001.
[6] E. Andò, Experimental study of the evolution of the microstructure of a granular medium under mechanical loading using tomography X-ray, PhD thesis, Laboratory 3SR, Grenoble, France, 2013.
[7] J. Baruchel, J.Y. Buffiere, E. Maire, X-ray tomography in material science. HERMES Science Publications, Paris, France, 2000.
[8] L.A. Feldkamp, L. C. Davis, J.W. Kress, Practical cone-beam algorithm. JOSA A 1(6) (1984) 612-619.
[9] M.A. Hashemi, G. Khaddour, B. Francois, T.J. Massart, S. Salager, A tomographic imagery segmentation methodology for three-phase geomaterials based on simultaneous region growing. Acta Geotechnica 9 (2014) 831–846.
[10] E. Bilotta, L. Cascini, V. Foresta, G. Sorbinow, Geotechnical characterisation of pyroclastic soils involved in huge flowslides. Geotechnical & Geological Engineering 23(4) (2005) 365-402.
[11] E. Bilotta, V. Foresta, G. Migliaro, The influence of suction on stiffness, shear strength, viscosity and collapse of some volcanic ashy soils. Proc. European Conference on Unsaturated Soils, 2–4 July, Durham UK, 2008, pp. 349–354.
[12] S. Cuomo, M. Della Sala, Rainfall-induced infiltration, runoff and failure in steep unsaturated shallow soil deposits. Engineering Geology. 162 (2013) 118-127.
[13] S. Cuomo, M. Moscariello, V. Foresta, Wetting simple shear tests on pyroclastic soils involved in shallow landslides Conference Proceedings 12Th International Symposium on Landslides (ISL) Napoli (Italy) 12-19, June 2016.
[14] M. Scheel, R. Seemann, M. Brinkmann, M. Di Michiel, A. Sheppard, S. Herminghaus, Liquid distribution and cohesion in wet granular assemblies beyond the capillary bridge regime. Journal of Physics: Condensed Matter 20(49) (2008) 494236.